

Control of synchronous motors with compensation of saturation effects

Dr.-Ing. Stephan Beineke, Dr.-Ing. Alexander Bähr, Dipl.-Ing. Fabian Mink LTi
DRIVES GmbH
Dr.-Ing. Radoslaw Nalepa, Moog GmbH

Control of synchronous motors with compensation of saturation effects

New developments of synchronous motors follow rigorous design rules to reduce manufacturing costs and to satisfy power density demands, therefore often enter saturation regions of the magnetic material. Saturation leads to inaccuracy in torque command or even instabilities in the current control loop. Respective compensation measures in speed and current control are presented for these commonly known effects. At high inverter output frequencies and high saturation levels another disturbance becomes significant. Harmonics in the flux distribution can cause high oscillations in the currents and the voltages leading to instability in the inner current control loop. As a countermeasure, the current controller is extended by an observer, which reduces significantly the oscillations.

Keywords: motor control, saturation, synchronous motors

1. Introduction

Permanent-magnet servomotors are the standard motors for demanding drive applications. In order to cut system costs, applications are increasingly seeking to use synchronous motor designs which have been optimised in terms of manufacturing cost and/or size. These particularly include motors with single-toothed windings which are frequency also designated as motors with "concentrated windings". Modelling of synchronous motors and coordinated controllers is usually based on the assumption of a fundamental wave model in which non-linear effects caused by saturation of the magnetic circuits in the motor resulting from the magnetic fields are ignored. In the case of the motor designs mentioned above, however, saturation effects occur which significantly influence the operating and control behaviour of the motor. So in future the saturation will need to be analysed in more detail than it has been to date, in order to control motors with a high degree of dynamism and to operate them at well above rated current. This paper sets out the main saturation effects and derives compensatory measures. These have been implemented in the software of the LTi DRIVES ServoOne servocontroller, and their efficacy has been demonstrated by measurement results. The measurements are performed on a MOOG G464 motor, which can be deployed in applications with a very high overload range. Its specifications are set out in table 1.

Table 1: Data sheet specifications for the MOOG G464 motor used

Rated current $I_N = 1.9\text{A}$	Rated torque $M_N = 1.12\text{Nm}$	Rated speed $n_N = 7400\text{ rpm}$
Inductances $L_d = L_q = 10.2\text{mH}$	Resistance $R = 9.8\Omega$	Flux linkage $\Psi = 0.052\text{Vs}$

2. Influence of saturation on motor inductance

The saturation behaviour of a motor can generally be described by the characteristics shown in figure 1. The magnetisation characteristic $\Psi(i_\mu)$ indicates the correlation between magnetic field strength and induction based on the variables magnetising current i_μ and flux linkage Ψ . The rise of the $\Psi(i_\mu)$ curve corresponds to an inductance. In this, a distinction must be made between the absolute amplitude inductance L_{amp} and the differential inductance $L_{diff}(i_\mu)$, corresponding to a derivation at a magnetic working point:

$$L_{amp}(i_\mu) = \Psi(i_\mu) / i_\mu \Leftrightarrow \Psi(i_\mu) = L_{amp} \cdot i_\mu$$

$$L_{diff}(i_\mu) = d\Psi(i_\mu) / di_\mu \quad (1)$$

Thus these functions can be mutually converted, as a result of which it is sufficient to determine one curve. Since the differential inductances for the motor are most easily measured with the aid of the drive controller, they are measured first. The measured characteristic of the differential inductance then, by integration, produces the functional characteristics for the flux linkage and the amplitude inductance. Figure 1 shows the measured dependency on the torque-forming q current, $L_{diff,q}(i_{Sq})$ and the flux linkage and amplitude inductance characteristics calculated from it.

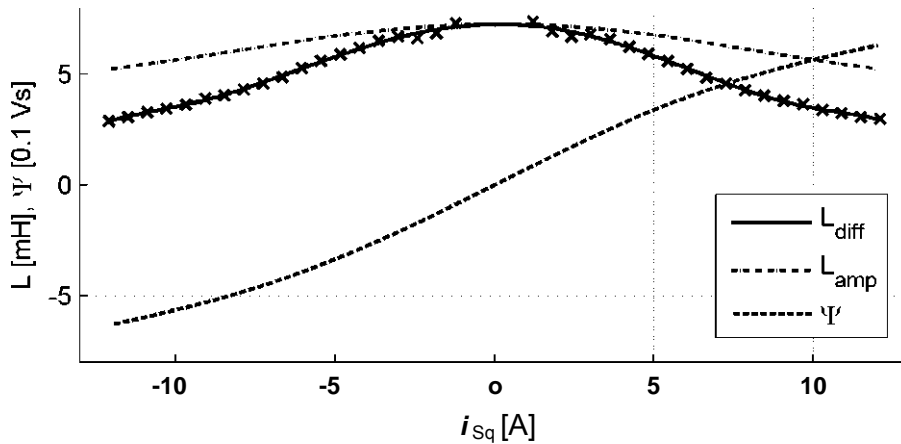


Figure 1: Measured dependencies of flux linkage, differential inductance and amplitude inductance on the q current

Since, firstly, the q current has to be provided with high dynamism and, secondly, on the synchronous machine in the overload range the q current can be many times the rated current, the characteristic of the differential inductance $L_{q,diff}(i_{Sq})$ is of particular importance to the dynamism of the current control loop, as referred to in chapter 4. By contrast, the amplitude inductance describes the dependency of the linked flux on the current. The result shown in figure 1 indicates that the characteristics for the amplitude inductance and differential inductance are symmetrical to the current $i_{Sq} = 0$. The flux linkage is presented on a different scale and is an uneven function of the q current, which is taken into account for derivation of the harmonic oscillations in chapter 5.

In the same way, the characteristics for the self-saturation ($L_q(i_{sq}), L_d(i_{sd})$) and the cross-saturation ($L_d(i_{sq}), L_q(i_{sd})$)¹ are determined for the motor and presented in figure 2. There is a noticeable shift in the characteristic $L_d(i_{sd})$ relative to the

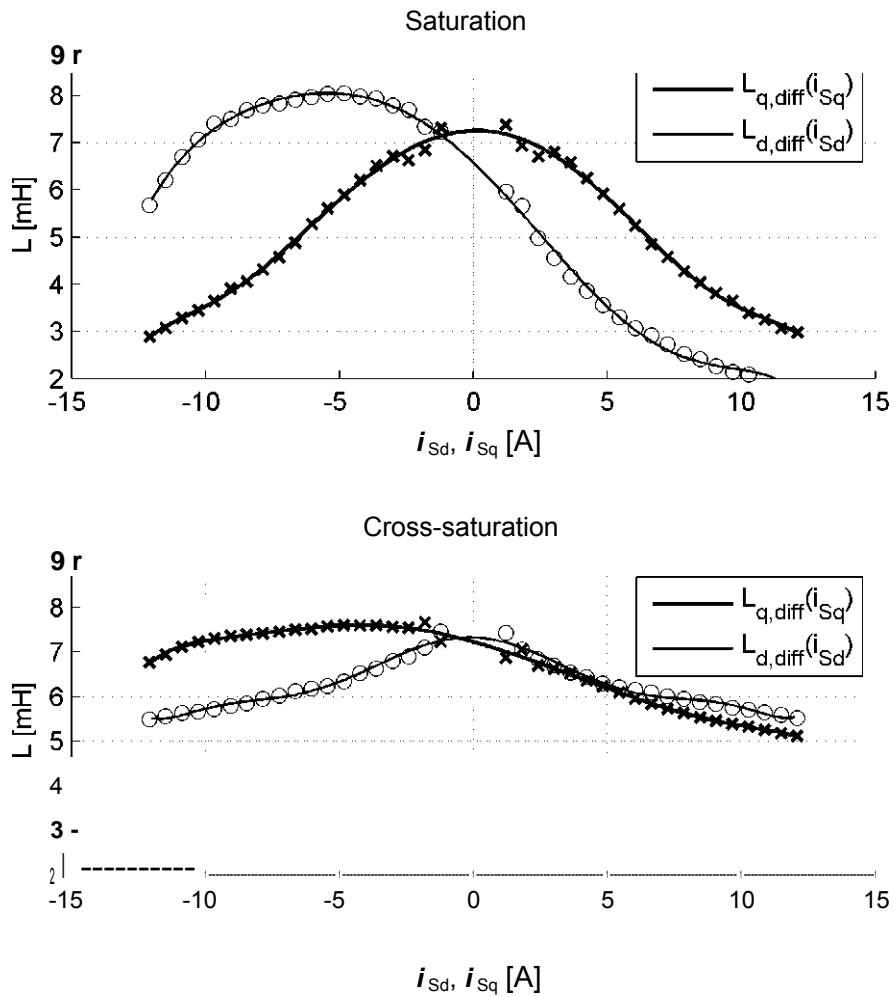


Figure 2: Characteristic of differential inductances for self-saturation and cross-saturation

characteristic $L_q(i_{sq})$ by a magnetising current which describes the magnetic bias due to the permanent magnets. Differences in inductance may also occur on the d and q axis because of differing gap heights. Usually synchronous machines are operated in the basic setting range without injection of a d current. In the field-weakening range a negative d current is injected, though this barely changes the inductance. In the event of significant overload (high q current) and a dynamic d current control, it may be necessary also to analyse the influence of cross-saturation on the d inductance.

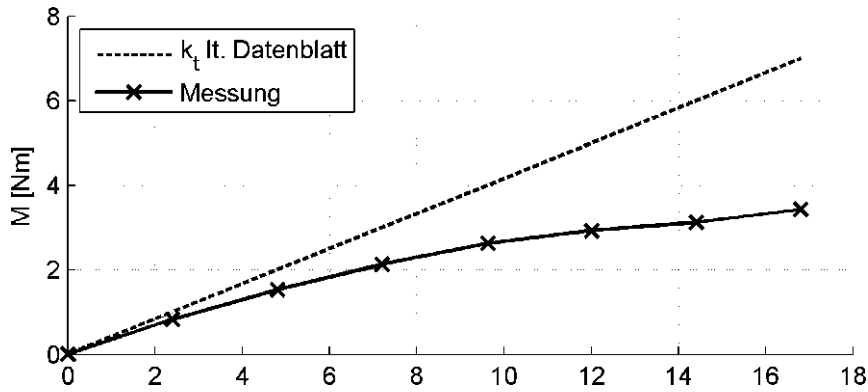
¹In the following the differential inductances are not separately labelled, i.e.

$$L_q = L_{q,diff} \text{ and } L_d = L_{d,diff}$$

3. Influence of saturation on the torque calculation

The effect of saturation on the reduction of the torque constant at higher motor current discussed in the following is well known.

Saturation results in a non-linear correlation between q current and torque. This correlation was determined for the motor under analysis on a test rig with a torque measurement shaft, and is indicated in figure 3. This characteristic can usually be made available by the motor manufacturer for each motor type in the form of a data sheet.



Legende:

----- k_t as per data sheet

Measurement

Figure 3: Measured motor characteristic $M = f_{Sat}(i_{Sq})$

This non-linearity may essentially have two disturbing effects for the drive solution if it is not allowed for by the drive controllers:

The saturation reduces the system gain in the speed control loop, resulting in an altered dynamic. Usually, however, this effect is only critical to control systems with highly dynamic settings in the high saturation range. If a linear correlation between current and torque is assumed, the torque is only precise as long as the motor is not saturated. In the saturation range an insufficient current is calculated for the required torque. As a result, the supplied torque becomes less than that required by the overlaid control system or the user. The maximum torque set by way of the torque limit parameter is also reduced. But in some applications, such as test rigs and position/force control systems in robotics or in fitness equipment, the drive demands precise torque actuals and limit values.

To compensate for the saturation, a torque calculator (see figure 4) is added to the control structure. The plotted motor characteristic $M = f_{Sat}(i_{Sq})$ is stored in the drive controller and the torque calculator calculates from the requested torque a corresponding setpoint value for the torque-forming q current based on the inversion function $i_{Sq} = f_{Sat}^{-1}(M)$.

The gain of the current controller is adapted dependent on the q current such that the variable system gain resulting from the saturation $1/L_q(i_{sq})$ is compensated. A subsequent 25% reduction in inductance, for example, results in a likewise 25% lower controller gain.

The efficacy of this measure is shown by figure 6. The current controller is rated for a specific dynamism, and the step response for currents in the range of the rated current i_{sqN} is plotted (6a). If a current is then set in the overload range (6b) with the same controller parameter settings, the increased system gain results in major overshoot or even instability in the control loop. The adaptation (6c) also results in good current control in terms of dynamism and stability in the overload range too.

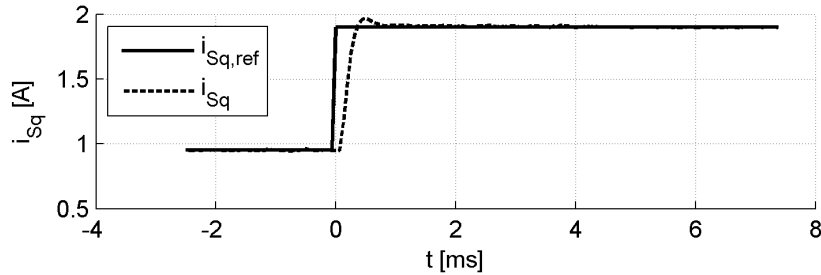


Figure 6a: Step response from $i_{sq} = 0,5 \cdot i_{sqN}$ auf $i_{sq} = i_{sqN}$ without adaptation

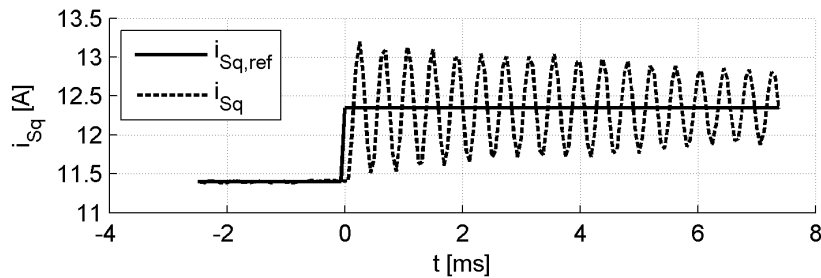


Figure 6b: Step response from $i_{sq} = 6 \cdot i_{sqN}$ auf $i_{sq} = 6,5 \cdot i_{sqN}$ without adaptation

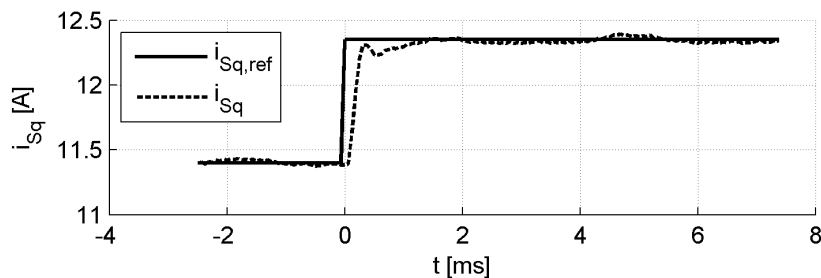


Figure 6c: Step response from $i_{sq} = 6 \cdot i_{sqN}$ auf $i_{sq} = 6,5 \cdot i_{sqN}$ with adaptation

5. Harmonic oscillations in the currents and voltages caused by saturation

Another effect of saturation that is rarely noticed in practice and paid little attention in the literature is the creation of harmonic oscillations in the stator currents and voltages. The starting point for the following observations was a demanding application in which a motor had to be accelerated very rapidly up to high speeds with 5 times the rated torque. Because of the 12-pole motor, this results in high supply frequencies. The corresponding run-up with the standard current control shown in figure 8 is presented in figure 10a. A sixth-harmonic oscillation is observed in the stator currents and voltages which only occurs to any marked extent at acceleration under 4 times overload or higher. Because the effect is load-sensitive, the inverter lockout times or a non-sinusoidal induced rotor voltage, which would likewise cause a sixth-harmonic interference voltage, are excluded as causes. The following observations provide a qualitative model by which the occurring oscillations can be explained. The sixth-harmonic oscillations can be derived from a model in which the saturation of the iron is not solely dependent on the

amount of the current space vector, but rather the stator flux components of each phase are essentially produced from the respective phase current by way of the saturation characteristic. For mathematical derivation, a three-phase current system is analysed in which a current space vector of amplitude i rotating at a radian frequency ω is injected. It is presumed that the correlation between flux and current is described by an uneven function, such as the function $\Psi(i_{sq})$ shown in figure 3. Then, when representing the string fluxes with the aid of a Fourier series, only the uneven Fourier coefficients are not equal to zero:

$$\begin{aligned} i_{sa} &= \Re(i \cdot e^{j\omega t}) \\ i_{sb} &= \Re(i \cdot e^{j\omega t + 2/3\pi}) \\ i_{sc} &= \Re(i \cdot e^{j\omega t + 4/3\pi}) \end{aligned}$$

 \Rightarrow

$$\begin{aligned} \Psi_{Sa} &= \Re\left(\sum_{k=1}^{\infty} \Psi_{2k-1} e^{j(2k-1)\omega t}\right) \\ \Psi_{Sb} &= \Re\left(\sum_{k=1}^{\infty} \Psi_{2k-1} e^{j(2k-1)(\omega t + 2/3\pi)}\right) \\ \Psi_{Sc} &= \Re\left(\sum_{k=1}^{\infty} \Psi_{2k-1} e^{j(2k-1)(\omega t + 4/3\pi)}\right) \end{aligned}$$

 (2)

On transformation into a two-string, stator-oriented α/β - coordinates system

- the harmonic oscillations with the ordinals $3k$ are eliminated if the individual motor phases are assumed to be symmetrical;
- the harmonic oscillations with the ordinals $6k-1$ produce a rotating field with a negative frequency;
- the harmonic oscillations with the ordinals $6k+1$ produce a rotating field with a positive frequency.

$$\underline{i}_S^S = i_{S\alpha} + j \cdot i_{S\beta} = \underline{i} \cdot e^{j\omega t} \Rightarrow \underline{\Psi}_S^S = \underline{\Psi}_1 e^{j\omega t} + \sum_{k=1}^{\infty} (\underline{\Psi}_{-(6k-1)} e^{-j(6k-1)\omega t} + \underline{\Psi}_{6k+1} e^{j(6k+1)\omega t}) \quad (3)$$

Transformation into a rotating d/q coordinates oriented to the rotor then respectively produces

- a fixed-position flux component corresponding to the fundamental model of the machine;
- a rotating field with a negative frequency (ordinals $6k$);
- a rotating field with a positive frequency (ordinals $6k$).

$$\underline{i}_S^R = i_{Sd} + j \cdot i_{Sq} = \underline{i}^R \Rightarrow \underline{\Psi}_S^R = \underline{\Psi}_1 + \sum_{k=1}^{\infty} (\underline{\Psi}_{-6k} e^{-j6k\omega t} + \underline{\Psi}_{6k} e^{j6k\omega t}) \quad (4)$$

Assuming sinusoidal phase currents, this model thus produces harmonic waves in the d/q flux distributions which cause sixth/twelfth/eighteenth harmonic oscillations in the d/q voltages referred to the supply frequency. Confirmation of this model is provided by the characteristic of the differential q inductance over the electrical angle shown in figure 7, which likewise has a corresponding sixth-harmonic wave L_{S6} which in turn is dependent on the q current.

The harmonic waves in the flux linkage also result in dominant sixth harmonics (and their harmonic oscillations) in the induced d/q phase voltages, whereby the voltage amount can be approximated by the equation:

$$\Delta u_{S6} = d\Psi_{S6} / dt = \omega_s \cdot L_{S6} \cdot i_{sq} \quad (5)$$

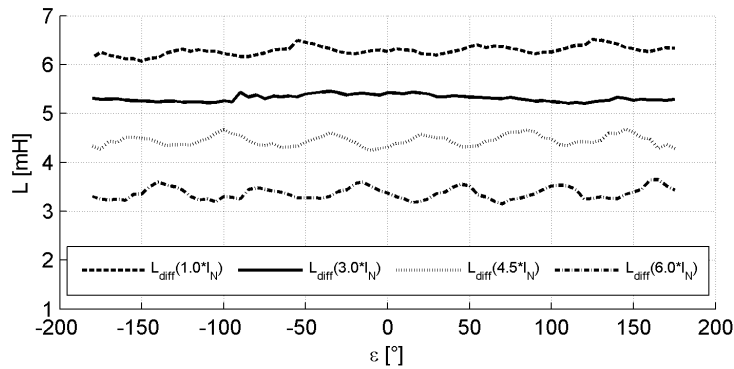


Figure 7: Characteristic of inductance on the q axis for various angles and currents

This model results in the conclusion that this effect occurs particularly markedly in practice in the following cases:

1. A sixth-harmonic oscillation can only occur at all if the saturation produces marked harmonic waves in the flux distribution. Thus the effect depends on the motor construction, and demonstrative analyses make it obvious that such conditions occur rather in concentrated windings than in distributed windings, and sixth-harmonic interference voltages are to be observed.
2. The effect occurs only when operating motors well above the rated current, because then the marked non-linearity between current and flux caused by saturation leads to a wide variation of the inductance L_{S6} and also the amount of the interference voltage Δu_{S6} rises proportionally to i_{Sq} .
3. The effect is particularly disturbing on the control behaviour at higher supply frequencies as, firstly, the amount of the interference voltage rises with the supply frequency ω_S and, secondly, the dynamism of the current control is then no longer sufficient to compensate for a sixth-harmonic electrical frequency disturbance.

The acceleration presented in figure 10a discussed at the beginning confirms these conclusions. Oscillations occur in the d and q currents and voltages as from a certain overload and speed. Whereas the current controller compensates for the oscillations at lower supply frequencies, at higher supply frequencies the isolation of the d and q current controller effected on computer can even mean that the current control becomes unstable. Owing to the effective dead time $T_{SUM,I}$ in the current controller and in view of the isolation, the high frequencies in the d/q currents mean that at a certain frequency the oscillations occurring in the current are fed-back with a positive sign and the current control rises. The effective dead time as shown in figure 8 results from the current measurement, the sample-and-hold operation based on the compensation implemented in the microcontroller and the pulse-width modulated actuator.

The acceleration measured with the observer is shown in figure 10b by way of comparison. The oscillations can be reduced to such an extent that the operation of the motor is no longer materially impaired by the saturation effects.

Figure 10a: Run-up with oscillations (without observer)

Figure 10b: Run-up without oscillations (with observer)

Legende:

soll = req [required]

6. Summary

The paper discussed major effects of saturation on permanently excited synchronous machines and set out the compensation functions integrated into the ServoOne drive controller. The non-linear correlation between q current and torque is taken into account in such a way that a required torque can be delivered precisely. The changing differential inductance results in a variable system gain in the current control loop, so that the gain of the controller has to be adapted.

Ultimately, the saturation also causes harmonic oscillations in the motor currents in operation with high overload and at high supply frequencies. A model was presented for this, describing the effects by means of a heuristic approach. With the aid of an observer structure the occurring harmonic oscillations can be greatly reduced. However, more extensive analysis is required in order to be able to model the observed behaviour fully and quantitatively .

Literature

- [1] Y. Murai, T. Watanabe, and H. Iwasaki: "Waveform distortion correction circuit for PWM inverters with switching lag-times," *IEEE Trans. Industrial Applications*, vol. 23, no. 5, pp. 881-886, 1987.
- [2] J. Holtz, L. Springob: "Identification and Compensation of Torque Ripple in High-Precision Permanent Magnet Motor Drives, *IEEE Trans. On Industrial Electronics*, vol. 43, no. 2, April 1996., pp. 309-320.
- [3] J.F. Moynihan, M.G. Egan, J.M.D. Murphy: "The Application of State Observers in Current Regulated PM Synchronous Drives", *Proceedings of IEEE IECON*, pp.20-25, 1994.